arXiv:1005.0284v1 [cond-mat.mes-hall] 3 May 2010

Effects of screened Coulomb impurities on autoionizing two-electron resonances in spherical quantum dots

Michael Genkin[1] and Eva Lindroth[1]

[1]*Atomic Physics, Stockholm University, AlbaNova, S-10691 Stockholm, Sweden*

(Dated: May 4, 2010)

Abstract

In a recent paper (Phys. Rev. B **78**, 075316 (2008)), Sajeev and Moiseyev demonstrated that the bound-to-resonant transitions and lifetimes of autoionizing states in spherical quantum dots can be controlled by varying the confinment strength. In the present paper, we report that such control can in some cases be compromised by the presence of Coulomb impurities. It is demonstrated that a screened Coulomb impurity placed in the vicinity of the dot center can lead to bound-to-resonant transitions and to avoided crossings-like behavior when the screening of the impurity charge is varied. It is argued that these properties also can have impact on electron transport through quantum dot arrays.

PACS numbers: 32.80.Zb, 73.21.La

I. INTRODUCTION

Autoionizing states have been very thoroughly investigated in conventional atomic systems. The accuracy achieved nowadays in experiment and theory is as high as to resolve hyperfine splittings in dielectronic resonances[1]. Another, currently very active, research topic involving autoionizing states are pump-and-probe experiments with short laser pulses, which make it possible to follow the autoionization process in real time and thus to resolve electron dynamics in atoms[2,3]. However, the autoionization process in artificial atoms like quantum dots is less known; From an experimental point of view, it is much more difficult to observe autoionization, since, contrary to "usual" atomic systems, quantum dots are imbedded into the semiconductor. The conventional atomic approach where autoionizing states are revealed as resonances in the cross section spectra for ionization by photon or particle impact is, in the case of quantum dots, not easily employed. Also theoretical data is rather scarce, since the confinment of the electrons in the dot is often modelled by a harmonic potential, which automatically excludes the possibility of resonances, while in reality the confining potential is, of course, finite. To circumvent this problem, other confinment models were suggested to study the autoionization process in two-electron quantum dots, like a finite well[4–6] or a Gaussian potential[7,8], which indeed led to interesting observations such as resonance-induced enhancement of the dot sensitivity to photons[8] or entanglement in resonances[6]. In the present work, we aim to study the effects of screened Coulomb impurities on the positions and lifetimes of such autoionizing resonances. The impact of charged impurities on the properties of quantum dots was addressed in connection with different confinment models, like a parabolic potential[9–12] or an infinite well[13] but also finite potentials[14–18]. Another interesting aspect is the behavior of quantum dots with impurities in external fields, which can give rise to effects like emergence of stable non-dispersive electron wave packets[19], field-enhanced electron localization[20] or change of optical properties[21]. However, we are only aware of one paper explicitly investigating the role of impurities in the autoionization process[4]. Therein, Buczko and Bassani considered a finite potential well with a hydrogenic impurity and chose an analytical method based on scattering theory techniques. Here, we adopt a different approach commonly known as "complex scaling" or "complex coordinate rotation" to determine the positions and widths of the resonances in a Gaussian-shaped spherical two-electron quantum dot with a Coulomb impurity. The method is described

in more detail in the following section II along with the computational procedure, and the results are presented in section III. A discussion and conclusions are given in section IV.

II. METHOD

The Hamiltonian of a spherical Gaussian two-electron quantum dot with a Coulomb impurity reads

$$H = -\sum_{i=1}^{2}\left(\frac{\hbar^2\nabla_{q_i}^2}{2m^*} + U_0 e^{-\alpha q_i^2} + \frac{\eta e^2}{4\pi\epsilon_0\epsilon q_i}\right) + \frac{e^2}{4\pi\epsilon_0\epsilon\left|\mathbf{q}_1 - \mathbf{q}_2\right|}, \tag{1}$$

where $\mathbf{q}_1, \mathbf{q}_2$ are the coordinates of the two electrons, m^* the effective electron mass, ϵ the dielectric constant of the semiconductor, U_0 the depth of the confining potential, α a parameter describing the range of the latter and η the effective charge of the impurity. For convenience, we introduce scaled parameters as suggested in Ref.[8]:

$$\begin{aligned} \mathbf{r}_i &= \frac{m^*}{m_e\epsilon}\mathbf{q}_i, \\ V_0 &= \frac{m_e\epsilon^2}{m^*}U_0, \\ \beta &= \frac{m_e^2\epsilon^2}{(m^*)^2}\alpha, \end{aligned} \tag{2}$$

where m_e is the electron mass, so that the Hamiltonian can be written as:

$$H = \frac{m^*}{m_e\epsilon^2}\left[-\sum_{i=1}^{2}\left(\frac{\hbar^2\nabla_{r_i}^2}{2m_e} + V_0 e^{-\beta r_i^2} + \frac{\eta e^2}{4\pi\epsilon_0 r_i}\right) + \frac{e^2}{4\pi\epsilon_0\left|\mathbf{r}_1 - \mathbf{r}_2\right|}\right]. \tag{3}$$

From here on, all quantities will be given in effective atomic units, and the values for the corresponding semiconductor can be reobtained from Eqs. (2). For example, in the case of GaAs we have $\epsilon = 12.4$ and $m^*/m_e = 0.067$, which gives the effective energy unit $1\,\mathrm{Ha}^* \approx 11.857\,\mathrm{meV}$ and the effective length unit $a_0^* \approx 9.794\,\mathrm{nm}$. To determine the bound as well as the resonant states of the system, we diagonalize the complex scaled Hamiltonian within a B-Spline basis set. This method was earlier applied to describe autoionizing resonances in atomic[22,23] and exotic[24–26] systems. The Hamiltonian (Eq.(3)) is dilation-analytic, so that the uniform complex scaling[27–30] of the coordinates can be imposed:

$$\mathbf{r}_i \to \mathbf{r}_i e^{i\theta}, \tag{4}$$

with a real parameter $0 < \theta < \pi/4$. The eigenvalues of the scaled Hamiltonian are complex. However, the physical states are invariant with respect to θ while pseudo-continuum states are rotated into the complex plane by the angle 2θ. After diagonalizing the scaled Hamiltonian for different values of θ, one obtains the bound states of the system as the eigenvalues with vanishing imaginary parts and the resonant states as complex eigenvalues,

$$E_{\mathrm{res}} = E_{\mathrm{pos}} - i\frac{\Gamma}{2}, \tag{5}$$

the real part of which gives the position of the resonance and the negative imaginary part the halfwidth of the latter. It is connected to the lifetime τ as $\tau = \hbar/\Gamma$. The diagonalization of the scaled Hamiltonian is carried out numerically using LAPACK-routines, and below we briefly describe the computational procedure. The radial part of the one-particle Hamiltonian h is given by

$$h = \frac{m^*}{m_e\epsilon^2}\left(-\frac{\hbar^2}{2m_e}\frac{\partial^2}{\partial r_i^2} + \frac{l_i(l_i+1)\hbar^2}{2m_e r_i^2} - V_0 e^{-\beta r_i^2} - \frac{\eta e^2}{4\pi\epsilon_0 r_i}\right), \tag{6}$$

and in the first step, the corresponding radial Schrödinger equation is solved in a sufficiently large box using piecewise polynomial functions B_k (so called B-Splines[31,32] of a certain order k) defined on a given knot sequence. Thus, the radial one-particle eigenfunctions φ_j are obtained in the form

$$\varphi_j(r) = \sum_k c_{kj} B_k(r) \tag{7}$$

with expansion coefficients c_{kj}. Subsequently, the matrix elements of the interaction potential

$$\frac{m_e\epsilon^2}{m^*}V_{12} = \frac{e^2}{4\pi\epsilon_0\left|\mathbf{r}_1 - \mathbf{r}_2\right|} \tag{8}$$

between the obtained states are computed using multipole expansion, where the radial integration can be carried out to machine accuracy using Gaussian quadrature, while the angular integration is performed analytically using Racah algebra[33]. The full Hamiltonian is then set up in the basis of coupled eigenstates to the one-particle Hamiltonians under consideration of the Pauli principle. Complex scaling is imposed by multiplying the kinetic terms by $\exp(-2i\theta)$ and the Coulomb-terms by $\exp(-i\theta)$. The real and imaginary part of the complex rotated Gaussian confining potential are given by

$$\mathrm{Re}\left[-V_0\exp\left(-\beta\left(r_i e^{i\theta}\right)^2\right)\right] = -V_0\exp\left(-\beta r_i^2\cos(2\theta)\right)\cos\left(\beta r_i^2\sin(2\theta)\right) \tag{9}$$

$$\mathrm{Im}\left[-V_0\exp\left(-\beta\left(r_i e^{i\theta}\right)^2\right)\right] = V_0\exp\left(-\beta r_i^2\cos(2\theta)\right)\sin\left(\beta r_i^2\sin(2\theta)\right) \tag{10}$$

and are scaled accordingly. After the setup of the Hamiltonian matrix is completed, the latter is diagonalized in the final step.

III. RESULTS

In the present calculations, we considered both donor and acceptor impurities, and therefore we varied the effective charge in the regions $\eta > 0$ and $\eta < 0$. This is a quite simple picture of the screening mechanism, but it should be sufficient to illustrate the effect of impurities on autoionizing states. In a more advanced approach, one could also include a possible spatial dependence of the screening. For example, Kwon[34] recently presented a model where the screening is modelled by an exponentially decreasing potential

$$V_{\rm imp}^{i} = \frac{q}{4\pi\epsilon\epsilon_0 r_i} \exp\left(-\frac{r_i}{r_s}\right), \tag{11}$$

where q is the true impurity charge and r_s the screening length which depends on the doping concentration in the semiconductor and the temperature (see Eqs.(9)-(15) in Ref.[34]). We simplify the treatment by varying η independently of r_i, as it is often done in atomic many-electron systems to model the screening effects by core electrons. Also, since we are mostly interested in autoionizing states which are situated not very close to the dot center, this approximation seems reasonable.

The parameters of the confining potential are chosen in the same region as suggested in Ref.[8]: throughout the calculations, the potential depth is kept fixed at $V_0 = 3\,\mathrm{Ha}^*$ and for the range parameter β we take certain values which are well suited to illustrate the physical behavior we aim to demostrate. To represent the basis states, a sequence of 48 knot points with a box size of $R = 24\,a_0^*$ is used to generate the B-Spline set, the order of which is $k = 7$ throughout the paper. We restrict our treatment to singlett resonances and include all configurations of $s-s, p-p$ and $d-d$ type for the ^1S symmetry and all configurations of $s-p$ and $p-d$ type for the ^1P symmetry, which is enough to reach sufficient convergence. The numerical stability of the method was confirmed by successfully reproducing the positions and widths of the resonances as given in Ref.[8] for the case $\eta = 0$ obtained with a Gaussian basis set. Figures 1 and 2 show the positions and halfwidths of the three lowest states and the $1s$-threshold for donor and acceptor impurities with different screening strengths. We observe that a donor impurity can turn an autoionizing state into a bound state, while for an

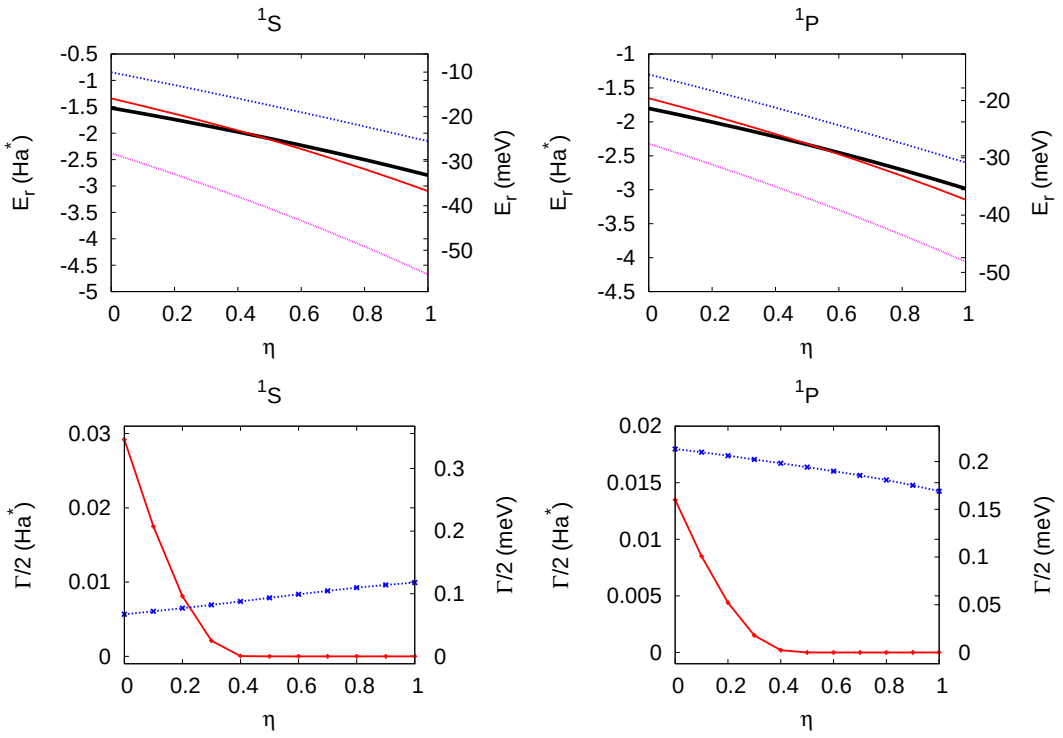

FIG. 1: (Color online) Donor impurity ($\eta > 0$). Upper panels: energy positions of the three lowest states (colored lines) and the position of the $1s$-threshold (solid black line) as the function of the screening strength, shown for ^1S (left) and ^1P (right) symmetry. Lower panels: Halfwidths of the occuring resonant states. As the position of the second state (red line) crosses the threshold, it becomes a bound state and its width vanishes. The values for the range parameter were taken as $\beta = 0.21\,(a_0^*)^{-2}$ for the ^1S symmetry and $\beta = 0.13\,(a_0^*)^{-2}$ for the ^1P symmetry. The energies and halfwidths are given both in scaled Hartree units (left axis) and meV (right axis) with material parameters of GaAs.

acceptor impurity the opposite behavior is seen. Somewhat similar situations are known to occur in atomic systems, when a certain electronic configuration gives or does not give rise to autoionizing resonances depending on the nuclear charge. For example, the $(1s^2 2p^2)^1S$ state is autoionizing in beryllium[35], while in the case of any other beryllium-like ion (e.g. beryllium-like carbon[36]) this state is bound. Of course, this analogy does not fully hold in the case studied here, since the confining potential remains unchanged, but to some extent it allows a qualitative insight in the observed behavior. Another interesting aspect in the case of donor impurities is that the width of the state which remains autoionizing (blue curve in Fig. 1) is affected differently for different total angular momenta: in the case of

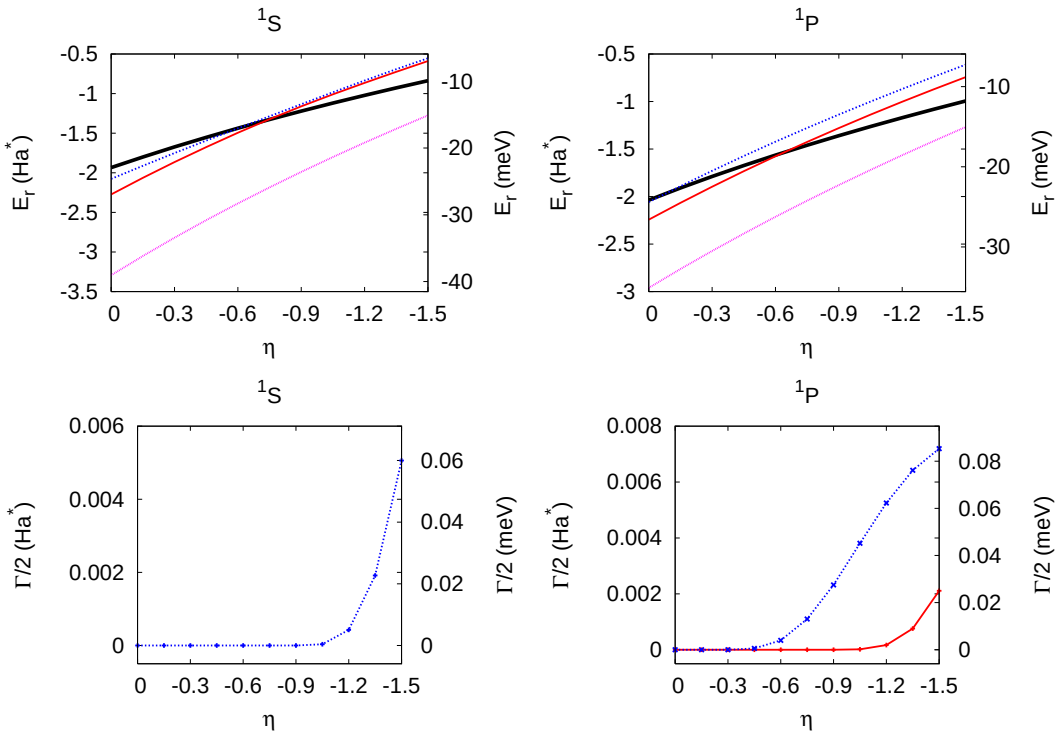

FIG. 2: (Color online) Same as in Fig. 1 for an acceptor impurity ($\eta < 0$). Here, we observe that two states (blue dotted and red solid lines) cross the threshold. However, in the case of ^1S symmetry, the width of the second state (red solid line) is orders of magnitude smaller than the one of the third state and is not shown in the plot since it is not distinguishable from zero on the given scale. The values for the range parameter were taken as $\beta = 0.10\,(a_0^*)^{-2}$ for the ^1S symmetry and $\beta = 0.08\,(a_0^*)^{-2}$ for the ^1P symmetry.

^1S symmetry it is slightly increasing while for the ^1P symmetry it is slightly decreasing as the effective impurity charge grows. Furthermore, we would like to point out that, for an acceptor impurity, the positions of the second and third states become very close to each other after crossing the threshold (blue and red curves in the upper left panel in Fig. 2). By "zooming in" into the relevant region, we see that these curves show an avoided-crossing like behavior. It is illustrated in Fig. 3, where we also plot the energy difference ΔE of the states vs. the effective impurity charge. To summarize, we observe that the dot spectra are quite sensitive with respect to impurities, both concerning the positions and, in case of autoionizing states, also the lifetimes, in particular because impurities can cause threshold-crossings so that bound states become resonant or vice versa. In the following section IV, we discuss the physical implications of the observed behavior which allows us to draw some

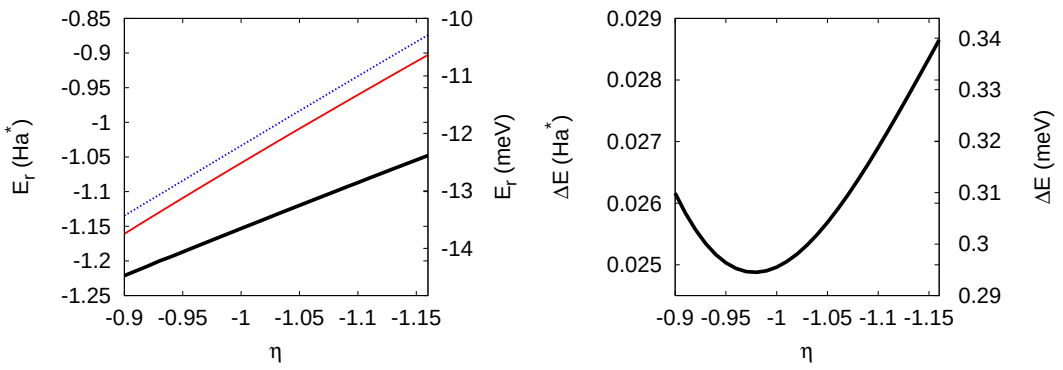

FIG. 3: (Color online) Left panel: "zoom-in" into the plot shown in the upper left panel of Fig. 2. Right panel: energy difference between the two states. The behavior is similiar to an avoided crossing. The range parameter of the confinment is $\beta = 0.10\,(a_0^*)^{-2}$

conclusions.

IV. DISCUSSION AND CONCLUSIONS

In the context of the presented results, we focus on two main topics in our discussion: resonance-enhanced sensitivity of the quantum dots to photons and the role of autoionizing resonances in transport processes through quantum dot chains. The practical purpose behind controlling the positions and lifetimes of resonances in quantum dots by adjusting the confining potential[8] was a possible application of the latter as sensitive photodetectors. As demonstrated therein, the presence of an autoionizing resonance leads, in fact, to a very significant increase of the photoionization rate, since autoionizing states can be intermediately populated in the photoionization process. Our results, however, indicate that in case of such an application attention should be paid to the purity of the semiconductor, since a donor impurity could turn an autoionizing state into a bound state which would considerably decrease the detector sensitivity. In other words, donor impurities counteract the controlled efficiency of such photodetectors. As for the role of acceptor impurities, we would like to mention their possible impact on electron transport through quantum dot chains. Let us for example imagine an array of quantum dots, prepared in a way that each of them initially contains one electron and consider the propagation of an electronic wave packet from one end of the chain to another[37]. If, in such a situation, acceptor impurities are present in one or several dots and give rise to autoionizing resonances, it could lead to

an additional channel for quantum transport where the electron is captured into a resonant state and remains there for a time span comparable to the lifetime of the resonance before it is released back to the continuum. This mechanism would thus compete with tunneling bewtween coupled quatum dots, possibly even giving rise to interference effects among the propagation paths. Qualitatively, one may even compare the situation to the first step in the process of dielectronic recombination in ions, when free electrons are captured into doubly excited states by simultaneous excitation of a core electron. Of course, in a semiconductor the resonant charecterstic would be less pronounced since the propagating electrons are not monochromatic; nevertheless, such a parallel between "usual" and artificial atoms is quite intriguing.

In conclusion, we studied autoionizing resonances in the presence of Coulomb impurities in spherical Gaussian-shaped two-electron quantum dots using the complex scaled direct diagonalization method. We found that donor impurities can turn resonant states with a finite lifetime into bound states, while acceptor impurities have the opposite effect. Implications of these features were discussed in the context of photoionization and transport processes in quantum dots, underlining the importance of the semiconductor purity in these particular applications.

Acknowledgements

We thank Prof. Nimrod Moiseyev for stimulating discussions during the 2009 meeting of the COST-action and Dr. Luca Argenti for helpful remarks. This work was financially supported by the Göran Gustafsson Foundation and the Swedish research council (VR).

---

[1] M. Lestinsky, E. Lindroth, D. A. Orlov, E. W. Schmidt, S. Schippers, S. Böhm, C. Brandau, F. Sprenger, A. S. Terekhov, A. Müller, et al., Phys. Rev. Lett. **100**, 033001 (2008).

[2] M. Uiberacker, T. Uphues, M. Schultze, A. J. Verhoef, V. Yakovlev, M. F. Kling, J. Rauschenberger, N. M. Kabachnik, H. Schröder, M. Lezius, et al., Nature **446**, 627 (2007).

[3] A. M. Zheltikov, A. A. Voronin, M. Kitzler, A. Baltuška, and M. Ivanov, Phys. Rev. Lett. **103**, 033901 (2009).

[4] R. Buczko and F. Bassani, Phys. Rev. B **54**, 2667 (1996).

[5] M. Bylicki, W. Jaskólski, A. Stachów, and J. Diaz, Phys. Rev. B **72**, 075434 (2005).

[6] A. Ferrón, O. Osenda, and P. Serra, Phys. Rev. A **79**, 032509 (2009).

[7] J. Adamowski, M. Sobkowicz, B. Szafran, and S. Bednarek, Phys. Rev. B **62**, 4234 (2000).

[8] Y. Sajeev and N. Moiseyev, Phys. Rev. B **78**, 075316 (2008).

[9] S. Mukhopadhyay and A. Chatterjee, Phys. Rev. B **55**, 9279 (1997).

[10] C. M. Lee, C. C. Lam, and S. W. Gu, Phys. Rev. B **61**, 10376 (2000).

[11] J. K. F. Yau and C. M. Lee, Phys. Rev. B **67**, 115321 (2003).

[12] M. Aichinger and E. Räsänen, Phys. Rev. B **71**, 165302 (2005).

[13] D. S. Chuu, C. M. Hsiao, and W. N. Mei, Phys. Rev. B **46**, 3898 (1992).

[14] R. K. Pandey, M. K. Harbola, and V. A. Singh, J. Phys.: Condens. Matter **16**, 1769 (2004).

[15] M. Şahin and M. Tomak, Phys. Rev. B **72**, 125323 (2005).

[16] H. A. Kassim, J. Phys.: Condens. Matter **19**, 036204 (2007).

[17] M. Şahin, Phys. Rev. B **77**, 045317 (2008).

[18] M. Şahin, Phys. Rev. B **77**, 119901(E) (2008).

[19] M. Kalinski, L. Hansen, and D. Farrelly, Phys. Rev. Lett. **95**, 103001 (2005).

[20] E. Lee, A. Puzder, M. Y. Chou, T. Uzer, and D. Farrelly, Phys. Rev. B **57**, 12281 (1998).

[21] S. Baskoutas, E. Paspalakis, and A. F. Terzis, J. Phys.: Condens. Matter **19**, 395024 (2007).

[22] N. Brandefelt and E. Lindroth, Phys. Rev. A **59**, 2691 (1999).

[23] N. Brandefelt and E. Lindroth, Phys. Rev. A **65**, 032503 (2002).

[24] M. Genkin and E. Lindroth, Eur. Phys. J. D **51**, 205 (2009).

[25] E. Lindroth, J. Wallenius, and S. Jonsell, Phys. Rev. A **68**, 032502 (2003).

[26] E. Lindroth, J. Wallenius, and S. Jonsell, Phys. Rev. A **69**, 059903(E) (2004).

[27] J. Aguilar and J. M. Combes, Commun. Math. Phys. **22**, 269 (1971).

[28] E. Balslev and J. M. Combes, Commun. Math. Phys. **22**, 280 (1971).

[29] B. Simon, Commun. Math. Phys. **27**, 1 (1972).

[30] N. Moiseyev, Phys. Rep. **302**, 212 (1998).

[31] C. deBoor, *A Practical Guide to Splines* (Springer Verlag, 1978).

[32] H. Bachau, E. Cormier, P. Decleva, J. E. Hansen, and F. Martin, Rep. Prog. Phys. **64**, 1815 (2001).

[33] I. Lindgren and J. Morrison, *Atomic Many-Body Theory* (Springer Verlag, 1986).

[34] Y. D. Kwon, Phys. Rev. B **73**, 165210 (2006).

[35] E. Lindroth and A. M. Mårtensson-Pendrill, Phys. Rev. A **53**, 3151 (1996).

[36] S. Mannervik, D. DeWitt, L. Engström, J. Lidberg, E. Lindroth, R. Schuch, and W. Zong, Phys. Rev. Lett. **81**, 313 (1998).

[37] G. M. Nikolopoulos, D. Petrosyan, and P. Lambropoulos, J. Phys.: Condens. Matter **16**, 4991 (2004).